Improvement of pseudorange measurements accuracy by using fast adaptive bandwidth lock loops

Fabrice Legrand, Christophe Macabiau, Jean-Luc Issler, Laurent Lestarquit, Christian Mehlen

Improvement Of Pseudorange Measurements Accuracy By Using Fast Adaptive Bandwidth Lock Loops

Fabrice Legrand, Christophe Macabiau, *CNS research laboratory of the ENAC*

Jean-Luc Issler, Laurent Lestarquit, *RadioNavigation Department of the CNES*

Christian Mehlen, *Alcatel Space Industries*

BIOGRAPHY

Fabrice Legrand is a Ph.D. candidate at the ENAC, in the CNS Research Laboratory. His thesis is supported by CNES and Alcatel Space Industries, and dedicated to radio navigation raw measurement integrity and accuracy improvements.
Christophe Macabiau is the head of Signal Processing Laboratory of the CNS Research Laboratory of the ENAC.
Jean-Luc Issler and Laurent Lestarquit are in the RadioNavigation Department at CNES. They are involved in the mission analysis and the development of STENTOR and DEMETER satellite GNSS receivers.
Christian Mehlen has been involved for ten years in study and development of GPS receivers at SEXTANT Avionique, and now at ALCATEL Space Industries. He is the technical responsible of TOPSTAR 3000, the spaceborne GPS receiver of ALCATEL.

ABSTRACT

The purpose of this paper is to present a new systematic, low cost and real-time adaptive algorithm to automatically set the loop filters parameters of the phase lock loops or delay lock loops used in synchronization systems like GPS. The aim of this method is to compute the loop filter coefficients which minimize the power of the thermal noise within the total tracking error, to improve the pseudorange measurements accuracy on each locked channel. Method is based on real-time estimations of the dynamics and signal-to-noise ratio of the incoming signals, which are used to compute the better compromise between the equivalent noise bandwidth and the steady state error factor of the loops. Estimates of signal parameters are obtained in real-time from observations of the error signal delivered by the dicriminator. From these estimates and from the knowledge of the equivalent linear model of the loop, an optimization function is built that gives the pole position of the loop transfer function that minimizes the equivalent noise bandwidth keeping a fixed probability that the error signal becomes greater than the lock threshold. This solution is evaluated by an iterative method with an update rate of 50 Hz or less, depending on the velocity of the variation of the dynamics and on the hardware constraints. The Fast Adaptive Bandwidth Lock Loop (FAB-LL) results in a real-time optimal use of the loops because it minimizes the power of the pseudorange measurement thermal noise with respect to the imposed error due to dynamics. Practical and theoretical approaches have shown the method is operational and robust.

INTRODUCTION

In radio navigation and localization systems, the technique to compute the position of a user is based on pseudorange measurements between several transmitters and the receiver. The receiver has to synchronize its own local replicas with the incoming signals to extract the navigation data and to perform the measurements. The most popular way to synchronize and to extract information from signals mixed with a carrier and pseudo-random binary sequences (PRN codes) in a noisy transmission channel context, is to use the common Phase and Delay Lock Loops (PLL and DLL) tracking systems. The most present sources of PLL and DLL synchronization error are the thermal noise, which is proportional to the Equivalent Noise Bandwidth (ENB) and is due to the noise on the transmission channel, and the dynamic stress error, which is conversely proportional to the ENB (see [1]). As these two error sources are conversely proportional, the common method to choose the ENB of the loop is to consider the worst cases of Signal-to-Noise Ratio (SNR) and dynamic of the incoming signal. This results in a sub-optimal use of the loops during periods where the dynamic is not maximal. The proposed algorithm adapts the ENB of the loop with respect to the real-time dynamic of the signal.
The first part of the paper describes a linearized model for common loops with integrate and dump predetection filters and provides the true analytic expressions of the synchronization error as a function of the poles of the transfer function of the loop. We derived from these expressions the Fast Adaptive Bandwidth (FAB) algorithm, which provided an optimal solution to adapt the loops to the signal as it is exposed in the second part of the paper. The last part deals with results of an initial implementation of the algorithm on a real GPS receiver.

I. LINEARIZED LOOPS MODELS

This section is divided in two parts. The first part deals with the linearized PLL model, and the second deals with the DLL model. Let's now consider the case of the PLL. LINDSEY and CHIE have derived digital linearized

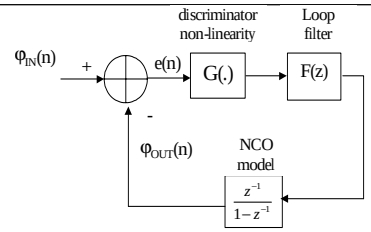

Figure I.1: Model of a digital PLL from LINDSEY and CHIE

models of various phase lock loops in [2]. The generic model is given in figure I.1. This model doesn't take into account of the effect of the predetection filters on the loop. As it is shown in figure I.2, the predetection filters are included in the feedback arm and they must not be ignored if the loop is set for high dynamics. Then we have

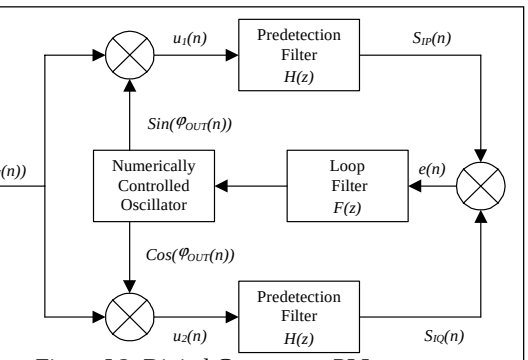

Figure I.2: Digital Costas type PLL

developed an extension to the generic model that includes the effects of predetection filters. If we derive the error signal of the Costas loop discriminator of figure I.2, we obtain:

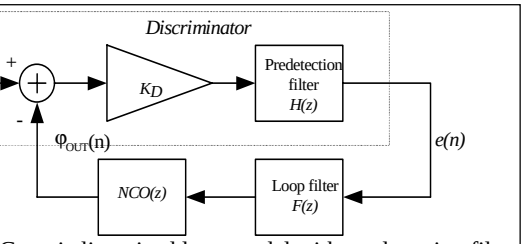

Figure I.3: Generic linearized loop model with predetection filter

$$e(n) = S_{IP}(n).S_{IQ}(n) = (u_1(n) * h(n)).(u_2(n) * h(n))$$

with

$$\begin{cases} u_1(n) = A.d(n).Sin(\varphi_{IN}(n)).Sin(\varphi_{OUT}(n)) \\ \quad = \dfrac{A.d(n)}{2}\left[Cos(\varphi_{IN}(n) - \varphi_{OUT}(n)) - Cos(\varphi_{IN}(n) + \varphi_{OUT}(n))\right] \end{cases} \quad (2)$$

$$\begin{cases} u_2(n) = A.d(n).Sin(\varphi_{IN}(n)).Cos(\varphi_{OUT}(n)) \\ \quad = \dfrac{A.d(n)}{2}\left[Sin(\varphi_{IN}(n) - \varphi_{OUT}(n)) + Sin(\varphi_{IN}(n) + \varphi_{OUT}(n))\right] \end{cases} \quad (3)$$

where *d(n)* is the sampled data. Suppose that the predetection filter suppresses the double frequency components and that the difference between the local phase and the received phase is small, then the cosine term is equivalent to 1 and the sine term is equivalent to the difference between the two phases. Under these assumptions, we can rewrite the in-phase and in-quadrature signals $S_{IP}(n)$ and $S_{IQ}(n)$ as:

$$\begin{cases} S_{IP}(n) = \dfrac{A.d(n)}{2} Cos(\varphi_{IN}(n) - \varphi_{OUT}(n)) * h(n) \\ \quad \approx \dfrac{A.d(n)}{2} * h(n) = \dfrac{A.d(n)}{2}\left|H(z)\right|_{z=1} = \dfrac{H_0.A.d(n)}{2} \end{cases} \quad (4)$$

$$\begin{cases} S_{IQ}(n) = \dfrac{A.d(n)}{2} Sin(\varphi_{IN}(n) - \varphi_{OUT}(n)) * h(n) \\ \quad \approx \dfrac{A.d(n)}{2} (\varphi_{IN}(n) - \varphi_{OUT}(n)) * h(n) \end{cases} \quad (5)$$

As the incoming sampled data *d(n)* is theoretically a succession of *+1* and *-1* values, the expression of the error signal becomes:

$$e(n) \approx \frac{H_0.A^2}{4} (\varphi_{IN}(n) - \varphi_{OUT}(n)) * h(n) \quad (6)$$

The result of (6) shows that the real phase error between the local and the incoming signals is filtered by the predetection filter to form the error signal of the loop. According to this, we can propose the generic linearized loop model of figure I.3. Most of receivers use integrate and dump (I&D) predetection filters. These filters perform an accumulation over a block of *Np* samples and output the sum with a rate *Np* times slower than the input rate. The length of the accumulation window *Np* corresponds to the ratio between the sampling frequency and the predetection bandwidth. This operation can be modeled in time by

$$Sum_{Np}(k) = \sum_{n=0}^{Np-1} u(k.Np - 1 - n) \quad (7)$$

We can rewrite it as

$$Sum_{Np}(k) = boxcar_{Np}(n) \otimes u(n)\Big|_{n=k.Np-1} \quad (8)$$

where *boxcar(n)* is the box function defined as

$$boxcar_{Np}(n) = \begin{cases} 0 & if \quad n < 0 \quad or \quad n \geq Np \\ 1 & if \quad 0 \leq n \leq Np - 1 \end{cases} \quad (9)$$

and where the symbol $\otimes$ represents the convolution operation. In conclusion, the I&D predetection filtering is equivalent to a convolution with the box function taken at epoch *k.Np-1*. Applying the I&D filter on the input signal is therefore equivalent to filter, delay and under-sample by *Np* as it is shown in figure I.4. The under-sampling operator is defined by

$$y_{under-sampled}(k) = y(n)\Big|_{n=k.Np} \quad (10)$$

In real receivers, the command signal of the NCO is held during all the predetection period. It means that we have to model the holding operation to complete the loop model. This operation can be modeled by an over-sampling convoluted with a box function, using the basic signal processing definition of the over-sampling that is

$$y_{over-sampled}(n) = \begin{cases} y\left(\dfrac{n}{Np}\right) & if \quad n = k.Np \quad (k \in \mathrm{N}) \\ 0 & otherwise \end{cases} \quad (11)$$

This model is shown on figure I.5. The inclusion of the I&D predetection filter model (figure I.4) and of the holding operation model (figure I.5) in the generic loop model of figure I.3 results, after simplifications shown in

appendix A of section V, on the model shown on figure I.6. This model can be split in two parts: an I&D filtering part and a closed loop part. The I&D filtering part performs the accumulation over a block of *Np* samples of

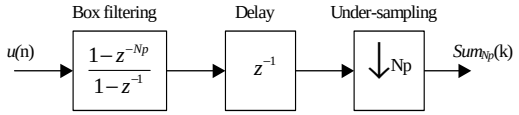

Figure I.4: Model of the I&D filter

the input phase, and the closed loop part is a well-known linear feedback system that can be characterized by its transfer function. Note that the closed loop part of the

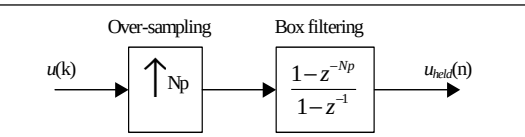

Figure I.5: Model of the holding operation

model differs from the model proposed by LINDSEY and CHIE in [2] (as represented on figure I.1): our model includes an additional delay in the feedback arm that models the effect of the predetection filters on the loop. Now, we have to derive some interesting properties of the model like the expressions of the transfer function, the ENB and the steady state error as a function of the loop filter parameters. From the scheme on figure I.6, we can

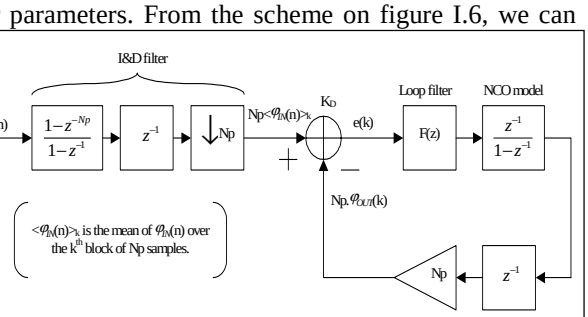

Figure I.6: Simplified digital model of the I&D PLL

write the transfer function of the loop $H(z)$ and the transfer function of the observable error $E(z)$ as a function of the mean value over the k^{th} block of *Np* samples of the real input phase define by

$$\langle \varphi_{IN}(n) \rangle_k = \frac{1}{Np} \sum_{n=0}^{Np-1} \varphi_{IN}(k.Np - 1 - n) \qquad (12)$$

These transfert functions are:

$$H(z) = TZ\left[\frac{\varphi_{OUT}(k)}{\langle \varphi_{IN}(n) \rangle_k} \right] = \frac{K_D.Np.F(z).z^{-2}}{1 - z^{-1} + K_D.Np.F(z).z^{-2}} \qquad (13)$$

and

$$E(z) = TZ\left[\frac{e(k)}{\langle \varphi_{IN}(n) \rangle_k} \right] = \frac{K_D.Np.(1 - z^{-1})}{1 - z^{-1} + K_D.Np.F(z).z^{-2}} \qquad (14)$$

Let's model the transfer function $F(z)$ of the loop filter as

$$F(z) = \frac{\sum_{n=0}^{N-2} b_n.z^{-n}}{(1 - z^{-1})^{N-2}} \qquad (15)$$

where $\{b_n\}$ are the coefficients of the filter, and N is the order of the transfer function of the loop. Loop filter is an N-2th order filter because of the presence of the additional unity delay in the feedback arm of the I&D loop model of figure I.6. Transient behaviors are modified but steady state behaviors are kept, as it will be shown later. It means that you always need to use a 1st order loop filter to track a 2nd order signal (constant phase acceleration produced by a constant radial acceleration of the receiver). We obtain the two transfer functions as a function of the loop filter coefficients by inserting (15) in (13) and (14):

$$H(z) = \frac{K_D.Np.\sum_{n=0}^{N-2} b_n.z^{-n-2}}{(1 - z^{-1})^{N-1} + K_D.Np.\sum_{n=0}^{N-2} b_n.z^{-n-2}} \qquad (16)$$

and

$$E(z) = \frac{K_D.Np.(1 - z^{-1})^{N-1}}{(1 - z^{-1})^{N-1} + K_D.Np.\sum_{n=0}^{N-2} b_n.z^{-n-2}} \qquad (17)$$

Note that

$$E(z) = K_D.Np.(1 - H(z)) \qquad (18)$$

Note that the two transfer functions on (16) and (17) have the same denominator of order *N*, so they also have the same poles. Let's note these *N* poles as $\{p_n\}_{n=1..N}$. Furthermore and for greater convenience, we will denote as *K* the constant product of the discriminator gain K_D with the integration length of the predetection filters *Np*. Then, equations (16) and (17) can be expressed as

$$E(z) = \frac{K.(1 - z^{-1})^{N-1}}{\prod_{n=1}^{N} (1 - p_n.z^{-1})} \qquad (19)$$

and (according to (18))

$$H(z) = 1 - \frac{E(z)}{K} \qquad (20)$$

The relations between the poles and the coefficients of the loop filter are obtained by identifying the denominators of (17) and (19). We have derived this calculation and the results for an N^{th} order loop are given in (21).

$$\begin{cases} K.b_0 = \sum_{\substack{k=1 \\ l \neq k}}^{N} p_k p_l - C_{N-1}^2; \quad K.b_1 = -\sum_{\substack{k=1 \\ l \neq k \\ m \neq l}}^{N} p_k p_l p_m + C_{N-1}^3; \\ \ldots; \quad K.b_{N-2} = (-1)^N.\prod_{k=1}^{N} p_k \end{cases} \qquad (21)$$

where

$$C_n^p = \frac{n!}{p!(n-p)!} \text{ and } K = K_D.Np \qquad (22)$$

Table 1 gives relations for useful orders. Note that the identification of the first order terms in (17) and (19) gives

Loop filter order	*Loop order*	*Loop filter coefficients*
0	2	$K.b_0 = p_1 p_2$
1	3	$K.b_0 = p_1 p_2 + p_1 p_3 + p_2 p_3 - 1$ $K.b_1 = -p_1 p_2 p_3$

Table 1: Relations between poles and loop filter coefficients for 2nd and 3rd order I&D-PLL

a characteristic property between the poles of the transfer function that is

$$\sum_{k=1}^{N} p_k = N - 1 \Rightarrow p_N = N - 1 - \sum_{k=1}^{N-1} p_k \qquad (23)$$

It means that the number of free setting poles is the same as the number of loop filter coefficients, which is *N*-1. We have derived the ENB and the steady state error of this linear system in the case of a setting of the *N*-1 poles as a unique multiple pole of order *N*-1. So let's define the value *p* of this multiple pole as:

$$p_k \Big|_{k=1\ldots N-1} = p \tag{24}$$

The value of the other pole is derived from (23), so

$$p_N = (N-1)(1-p) \tag{25}$$

With this setting, the transfer function of the observable error is (from (24), (25) and (19)):

$$E(z) = \frac{K.\left(1-z^{-1}\right)^{N-1}}{\left(1-p.z^{-1}\right)^{N-1}\left(1-(N-1)(1-p).z^{-1}\right)} \tag{26}$$

The stability of this system implies that its poles are in the unity circle of the *z*-plane. So, the system is stable if

$$\begin{cases} -1 < p < 1 \\ and \\ -1 < (N-1)(1-p) < 1 \end{cases} \Leftrightarrow \frac{N-2}{N-1} < p < 1 \tag{27}$$

The normalized equivalent noise bandwidth B_L is usually defined as:

$$B_L = \frac{\|H(z)\|_2^2}{2} \tag{28}$$

where

$$\|H(z)\|_2^2 = \frac{1}{2\pi j}\oint_{|z|=1} H(z).H(z^{-1}).\frac{dz}{z} \tag{29}$$

To compute the ENB as a function of the multiple pole *p* of the loop, it is better to compute B_L as a function of the squared norm of the error transfer function *E(z)*. According to (18) and (29), we have

$$\|E(z)\|_2^2 = \frac{K^2}{2\pi j}\oint_{|z|=1} (1-H(z)).(1-H(z^{-1})).\frac{dz}{z} \tag{30}$$

As *H*(z) is a low-pass filter, we shown that

$$\|E(z)\|_2^2 = K^2.(1+\|H(z)\|_2^2) \tag{31}$$

and consequently (from (28) and (31)):

$$B_L = \frac{1}{2}\left(\frac{\|E(z)\|_2^2}{K^2} - 1\right) \tag{32}$$

Note that this bandwidth is normalized by the sample rate of the loop. You have to multiply B_L by the 50Hz frequency to obtain the bandwidth in Hertz unit. The

Loop filter order	*Loop order*	$\|E(z)\|_2^2$
0	2	$\frac{2K^2}{2-p+2p^3-p^4}$
1	3	$\frac{2K^2.(6p^2-3p+1)}{(p+1)^3.(3-2p).(1-2p+2p^2)^2}$

Table 2: Squared norm of the observable error transfer function of an I&D PLL as a function of the multiple pole of the transfer function.

squared norm of *E*(z) as a function of the multiple pole *p* defined in (24) has been derived for several usual order loops in table 2. The corresponding normalized loop bandwidths have been plotted on figure I.7. The equivalent phase thermal noise at the input of a Costas loop is usually modeled (see [1]) by a white noise with a power of

$$\sigma_{b_{IN}}{}^2 = \frac{F_S}{2.C/N_0}\left(1+\frac{Bp}{2.C/N_0}\right) \tag{33}$$

where F_S is the sampling frequency. This expression is

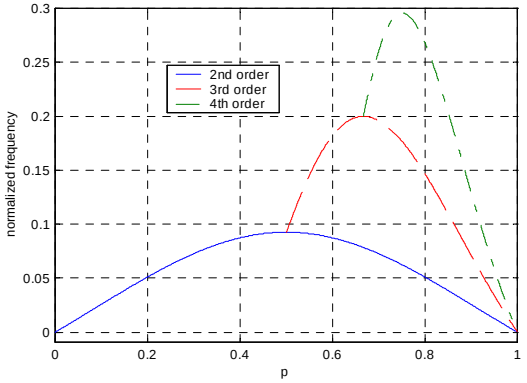

Figure I.7: Normalized ENB of I&D-PLL of order 2, 3 and 4 (in their stability range)

obtained by analyzing the effect of the noise in the discriminator using the narrow-band noise decomposition theory of RICE (see [1]), and is the power of the phase thermal noise at the input of our model. The term in bracket in (33) is due to the squaring losses. Then, the noise at the input of the filter *H*(z) defined in (13) is the mean value of the equivalent phase thermal noise as defined in (12). Its power is then

$$\sigma_{\langle b_{IN}\rangle}{}^2 = \frac{\sigma_{b_{IN}}{}^2}{Np} \tag{34}$$

The ratio between the sampling frequency and the length of the predetection window *Np* is exactly equal to the predetection bandwidth (in Hertz unit) *Bp*. Then, the total power of the thermal noise on the output phase of the NCO is

$$\sigma_{b_{OUT}}{}^2 = \frac{B_L.B_p}{C/N_0}\left(1+\frac{Bp}{2.C/N_0}\right) \text{ (in } rad^2\text{)} \tag{35}$$

where B_L is the ENB in normalized frequency unit and B_p is the predetection bandwidth in Hertz unit. This result is coherent with the usual expression of the total error power due to thermal noise (cf [3] for example). Note that this model of noise neglects the effect of the phase noise produced by the NCO. In reality, the NCO phase noise cannot be neglected if the loop has a very narrow bandwidth. The steady state error depends on the order of the loop and on the input phase of the signal. Suppose that the phase of the baseband input signal is given by

$$\varphi_{IN}(t) = \sum_{m=0}^{\infty}\varphi_0^{(m)}.\frac{t^m}{m!} \tag{36}$$

where $\varphi_0^{(m)}$ is the initial value of the mth derivative of the input phase. Its sampled version is then

$$\varphi_{IN}(n) = \sum_{m=0}^{\infty}\varphi_0^{(m)}.\frac{n^m}{m!.F_S{}^m} \tag{37}$$

where F_s is the sampling frequency. As it is derived in annex B of section V, the mean value over the k^{th} block of Np sample of the input phase is

$$\langle \varphi_{IN}(n) \rangle_k = \sum_{m=0}^{\infty} A_0^{(m)} . \frac{k^m}{m!} \qquad (38)$$

where $A_0^{(m)}$ is the equivalent initial value of the mth derivative of the meaning input phase. It is also shown in

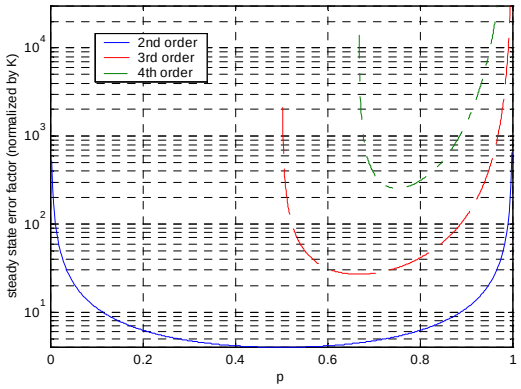

Figure I.8: Steady state error factor normalized by K of I&D-PLL of order 2, 3 and 4 (in their stability range), in the case of a multiple pole of order N-1

annex B that $A_0^{(m)}$ can be approximated by

$$A_0^{(m)} \approx \frac{\varphi_0^{(m)}}{B_p{}^m} \qquad (39)$$

Then, the steady state error of the system is given by this particular property of the z-transform (see [4]):

$$E_\infty = \lim_{z \to 1} \left\{ (z-1).E(z).TZ\left[\langle \varphi_{IN}(n) \rangle_k \right] \right\} \qquad (40)$$

$$\Leftrightarrow$$

$$E_\infty = \sum_{m=0}^{\infty} \frac{A_0^{(m)}}{m!} \lim_{z \to 1} \left\{ (z-1).E(z).TZ\left[k^m \right] \right\} \qquad (41)$$

If we derived (41) with the expression of E(z) for an N^{th} order loop given in (19), we find that the terms whose order is smaller than N-1 are equal to zero (the error converges towards zero), the ones whose order is greater than N-1 tend towards infinity (the loop diverges), and the term of order N-1 is a constant. It means that an N^{th} loop can track an input phase of order N-1 with a steady state error of

$$E_\infty = \frac{K.A_0^{(N-1)}}{\prod_{n=1}^{N} (1 - p_n)} \qquad (42)$$

Let's define the steady state error factor G as the ratio between the steady state error E_∞ and the equivalent N-1th derivative of the meaning input phase $A_0^{(N-1)}$ as

$$G = \frac{E_\infty}{A_0^{(N-1)}} = \frac{K}{\prod_{n=1}^{N} (1 - p_n)} \qquad (43)$$

The steady state error factor (SSEF) has been plotted on figure I.8 for several order loops in the case of the multiple pole p of order N-1 defined in (24) and (25). Note that the ENB (figure I.7) and the SSEF (figure I.8) are conversely proportional.

Let's now introduce the second part of this section that deals with the DLL model. The generic scheme of a DLL

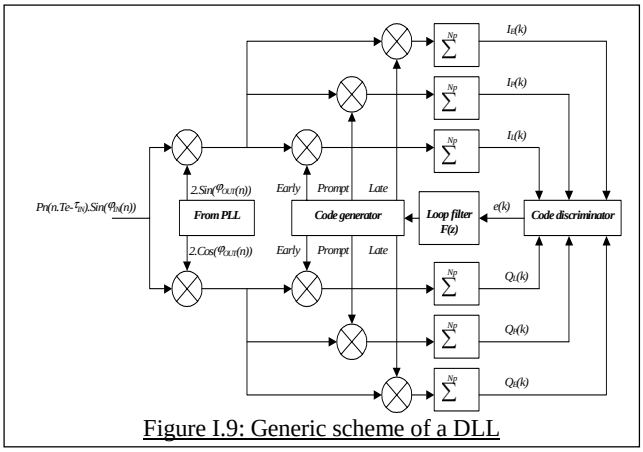

Figure I.9: Generic scheme of a DLL

is shown on figure I.9. where

$$I_L(k) = R_{pn}\left(\tau_{IN} - \tau_{OUT} - \frac{d}{2} \right).Cos\left(\langle \varphi_{IN}(n) \rangle_k - \varphi_{OUT}(k) \right)$$

$$I_E(k) = R_{pn}\left(\tau_{IN} - \tau_{OUT} + \frac{d}{2} \right).Cos\left(\langle \varphi_{IN}(n) \rangle_k - \varphi_{OUT}(k) \right)$$

$$I_P(k) = R_{pn}\left(\tau_{IN} - \tau_{OUT} \right).Cos\left(\langle \varphi_{IN}(n) \rangle_k - \varphi_{OUT}(k) \right)$$

$$Q_L(k) = R_{pn}\left(\tau_{IN} - \tau_{OUT} - \frac{d}{2} \right).Sin\left(\langle \varphi_{IN}(n) \rangle_k - \varphi_{OUT}(k) \right)$$

$$Q_E(k) = R_{pn}\left(\tau_{IN} - \tau_{OUT} + \frac{d}{2} \right).Sin\left(\langle \varphi_{IN}(n) \rangle_k - \varphi_{OUT}(k) \right)$$

$$Q_P(k) = R_{pn}\left(\tau_{IN} - \tau_{OUT} \right).Sin\left(\langle \varphi_{IN}(n) \rangle_k - \varphi_{OUT}(k) \right)$$

and where d is the delay between the early and the late channel, τ_{IN} is the delay of the input code, and τ_{OUT} is the delay of the prompt locally generated code. Note that these expressions are only true if we consider that the delay of the input code is relatively constant during the predetection time interval. The code discriminator forms the error signal by differencing early and late correlation functions (see [3]). As an example, the coherent early minus late discriminator is define as:

$$e(k) = \left(I_E(k) - I_L(k) \right) sign\left(I_p \right)$$

Each discriminator has a linear range. For example, the discrimination function of the early minus late is linear in the range [-d/2, d/2]. In its linear range, the gain of this discriminator is

$$K_D = \frac{-2}{Tc}$$

where Tc is the duration of a code chip. In its linear range, the DLL can be modeled as shown on figure I.10. The local code generator is modeled as a digital integrator as the NCO in the case of the PLL (see [1]). As for the PLL, we can derive the expressions of the transfer function, the ENB and the steady state error of the loop as a function of the loop filter. The transfer function of the loop is

$$H(z) = \frac{Tz[\tau_{OUT}(k)]}{Tz[\tau_{IN}(k)]} = \frac{K_D.F(z).z^{-1}}{1 + (K_D.F(z) - 1).z^{-1}} \qquad (44)$$

The transfer function of the observable error is given by

$$E(z) = \frac{Tz[e(k)]}{Tz[\tau_{IN}(k)]} = \frac{K_D.(1-z^{-1})}{1+(K_D.F(z)-1).z^{-1}} \quad (45)$$

Note that

$$H(z) = 1 - \frac{E(z)}{K_D} \quad (46)$$

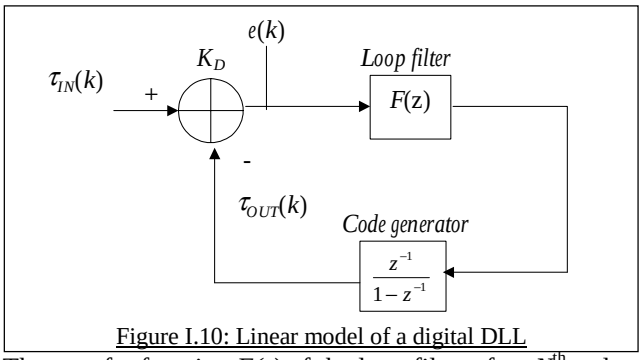

Figure I.10: Linear model of a digital DLL

The transfer function *F(z)* of the loop filter of an N^{th} order DLL is modeled as

$$F(z) = \frac{\sum_{n=0}^{N-1} b_n.z^{-n}}{(1-z^{-1})^{N-1}} \quad (47)$$

Then the transfer functions can be denote as a function of the coefficients of the loop filter as

$$H(z) = \frac{K_D.\sum_{k=0}^{N-1} b_k.z^{-k-1}}{(1-z^{-1})^N + K_D.\sum_{k=0}^{N-1} b_k.z^{-k-1}} \quad (48)$$

and

$$E(z) = \frac{K_D.(1-z^{-1})^N}{(1-z^{-1})^N + K_D.\sum_{k=0}^{N-1} b_k.z^{-k-1}} \quad (49)$$

Let's note the *N* poles of these transfer functions as $\{p_n\}_{n=1..N}$. Then

$$E(z) = \frac{K_D.(1-z^{-1})^N}{\prod_{n=1}^{N}(1-p_n.z^{-1})} \quad (50)$$

The relations between the poles of the transfer function and the coefficients of the loop filter are obtained by developing and identifying the denominators of (49) and (50). Then, for an N^{th} order DLL, these relations are

$$\begin{cases} K_D.b_0 = -\sum_{k=1}^{N} p_k + N; \quad K_D.b_1 = \sum_{\substack{k=1 \\ l\neq k}}^{N} p_k p_l - C_{N-1}^2; \\ K_D.b_2 = -\sum_{\substack{k=1 \\ l\neq k \\ m\neq l}}^{N} p_k p_l p_m + C_{N-1}^3; \cdots; K_D.b_{N-1} = (-1)^N.\left(\prod_{k=1}^{N} p_k - 1\right) \end{cases} \quad (51)$$

where

$$C_n^p = \frac{n!}{p!(n-p)!} \quad (52)$$

Table 3 gives relations for useful orders. Then, we have derived expressions of the ENB and of the steady state error of the DLL in the case of a setting of the *N* poles as a unique multiple pole of order *N*. This pole is define as

$$p_k \big|_{k=1...N} = p \quad (53)$$

Then, the stability of the system imposes that

$$|p| < 1 \quad (54)$$

The ENB is defined in (28) and (29). The relation between

Loop filter order	*Loop order*	*Loop filter coefficients*
0	1	$K.b_0 = 1 - p_1$
1	2	$K.b_0 = 2 - (p_1 + p_2)$ $K.b_1 = p_1 p_2 - 1$

Table 3: Relations between poles and loop filter coefficients for DLL of order 1 and 2

the squared norm of *H*(z) and *E*(z) in (32) is also true for the DLL, with K_D instead of *K*. Computed results for 1st and 2nd order loops are given in table 4, and the corresponding ENB are plotted on figure I.11. The power of the thermal noise tracking error is

$$\sigma_{b_{OUT}}{}^2 = \sigma_{b_{IN}}{}^2.B_L.Bp \quad (55)$$

where B_L is the ENB in normalized frequency, *Bp* is the

Loop order	$\|E(z)\|_2^2$
1	$\frac{2K_D{}^2}{p+1}$
2	$\frac{2K_D{}^2.(p+3)}{(p+1)^3}$

Table 4: Squared norm of the observable error transfer function of a DLL as a function of the multiple pole of the transfer

predetection bandwidth and $\sigma_{b_{IN}}{}^2$ is the power of the equivalent code phase thermal noise of the input signal of the loop. As an example, this value is

$$\sigma_{b_{IN}}{}^2 \approx \frac{d}{2C/N_0} \quad (56)$$

for the coherent discriminator, $\sigma_{b_{IN}}{}^2$ is in squared units of chips and the delay *d* between the early and late channels is also in units of chips. This variance is converted in squared seconds by multiplying its expression by the squared duration of a chip. To derive the steady state error, let's consider that the input PRN code delay is composed by the sum of different order components. So

$$\tau_{IN}(t) = \sum_{m=0}^{\infty} \tau_0^{(m)}.\frac{t^m}{m!} \quad (57)$$

where $\tau_0^{(m)}$ is the initial value of the mth derivative of the input code delay. Under the assumption that this delay is relatively constant during the predetection period, its sampled version at the output of the I&D filters is then

$$\tau_{IN}(k) = \sum_{m=0}^{\infty} A_0^{(m)}.\frac{k^m}{m!} \quad (58)$$

where $A_0^{(m)}$ is the equivalent mth derivative coefficient of the input code delay defined by

$$A_0^{(m)} = \frac{\tau_0^{(m)}}{B_p{}^m} \quad (59)$$

Then, the steady state error is done by

$$E_\infty = \lim_{z\to 1}\{(z-1).E(z).TZ[\tau_{IN}(k)]\} \quad (60)$$

⇔

$$E_\infty = \sum_{m=0}^{\infty} \frac{A_0^{(m)}}{m!} \lim_{z\to 1}\left\{(z-1).E(z).TZ\left[k^m\right]\right\} \qquad (61)$$

If we derived (61) with the expression of $E(z)$ for an N^{th} order loop given in (50), we find that the terms of (61) whose order is smaller than N are equal to zero (the error

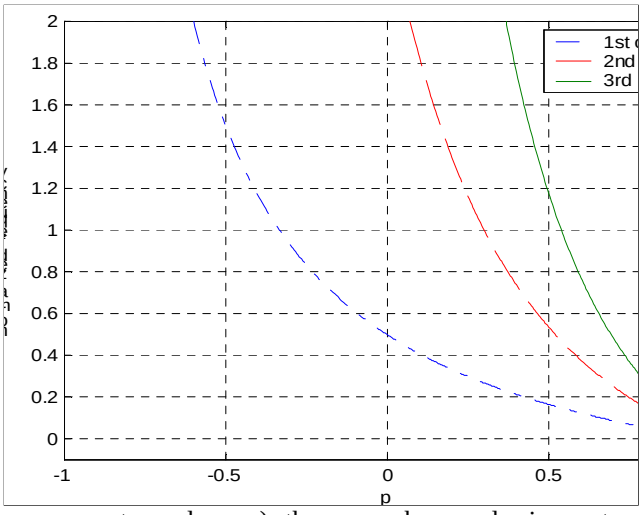

converges towards zero), the ones whose order is greater than N tend towards infinity (the loop diverges), and the term of order N is a constant. It means that an N^{th} order loop can track an input code delay of order N with a steady state error of

$$E_\infty = \frac{K_D.A_0^{(N)}}{\prod_{n=1}^{N}(1-p_n)} \qquad (62)$$

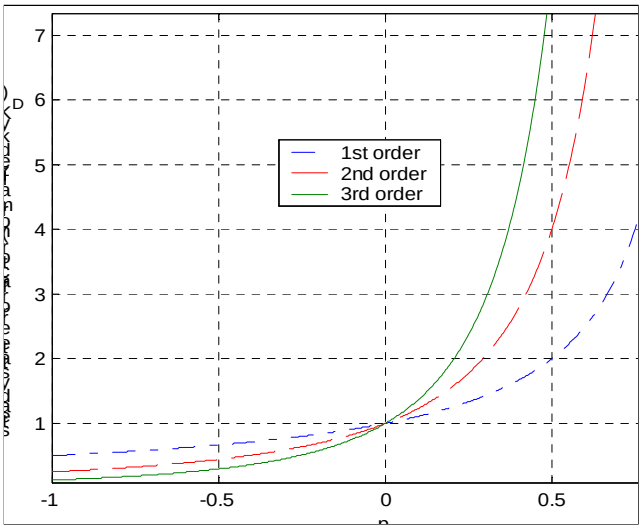

As for the PLL, we can define the steady state error factor G of the DLL as the ratio between the steady state error value by the equivalent N^{th} derivative of the input code delay, so

$$G = \frac{E_\infty}{A_0^{(N)}} = \frac{K_D}{\prod_{n=1}^{N}(1-p_n)} \qquad (63)$$

The SSEF has been plotted on figure I.12 for several order loops in the case of the multiple pole p of order N defined in (53).

II. FAST ADAPTIVE BANDWIDTH LOCK LOOP ALGORITHM

In this section, we describe how the FAB algorithm computes a real-time optimal solution for the parameters of the loop. Note that this theory is just as valid for the PLL as for the DLL by substituting the appropriate model described in section I in the following development. The aim of the FAB algorithm is to compute in real-time the optimal multiple pole of the transfer function of the loop that minimizes the thermal noise on the measurements by taking account of the steady state error due to dynamic. Let's consider the observable error signal $e(k)$ at the output of the discriminator. Assuming that the main sources of error are the thermal noise and the steady state error, we can model $e(k)$ as the sum of these two contributions:

$$e(k) = b(k) + E_\infty(k) \qquad (64)$$

where $b(k)$ is a zero mean value gaussian noise with a standard deviation σ_b of

$$\sigma_b = \sqrt{\left\|E(z,p)\right\|_2^2}.\sigma_{eq} \qquad (65)$$

where $E(z,p)$ is the transfer function of the observable error as defined in section I by (14) for the PLL and by (44) for the DLL, and where σ_{eq} is the standard deviation of the equivalent gaussian carrier phase or code delay thermal noise at the input of the loop, as also defined in section I by (33) for the PLL and by (56) for the DLL. $E_\infty(k)$ is the steady state error at epoch k, and

$$E_\infty(k) = A_{IN}(k).G(p) \qquad (66)$$

where $A_{IN}(k)$ is the N-1th derivative of the equivalent input carrier phase (see (39)) or the N^{th} derivative of the equivalent input code delay (see (59)) and $G(p)$ is the steady state error factor (SSEF) as defined in chapter I. The error signal is then a gaussian noise with an instantaneous mean value of $E_\infty(k)$ and a standard deviation of σ_b. To perform good pseudorange or carrier phase measurements, it is better to minimize the power of the random part of the error. But minimizing the power of the random part of the error results in an increasing of its mean value because the squared norm of $E(z,p)$ and the ENB are conversely proportional with the SSEF as it was shown in section I. Moreover, we must be careful that the error signal doesn't leave the lock range of the discriminator. This lock range depends on the discriminator used in the loop. Let's note the lock range of the discriminator as

$$\text{Lock Range} = [-L_{th}, L_{th}]$$

and let's fixe the probability P_0 that the error signal takes values outside the lock range as

$$P_0 = prob[\ |e(k)| \geq L_{th}\ ] \qquad (67)$$

As the statistic law of the error signal is gaussian, then (67) is equivalent to

$$P_0 = prob[\ |e(k)| \geq |E_\infty(k)| + a.\sigma_b\ ] \qquad (68)$$

where a is a function of P_0, $E_\infty(k)$ and σ_b and is defined by

$$\int_{|E_\infty|+a.\sigma_b}^{\infty} \frac{1}{\sigma_b.\sqrt{2\pi}} \cdot e^{\frac{(x-|E_\infty|)^2}{2.\sigma_b^2}} dx = P_0 \qquad (69)$$

For example, if we take a equal to 1, then (69) gives a probability P_0 that the error signal be out of the lock range

of 0.16, if a equal 2 then the probability is 0.02, and if a equal 3 the probability will be 0.001. Then, from (67) and

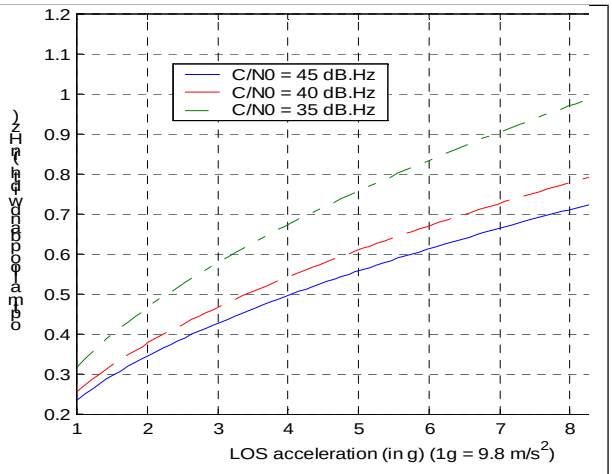

(a)

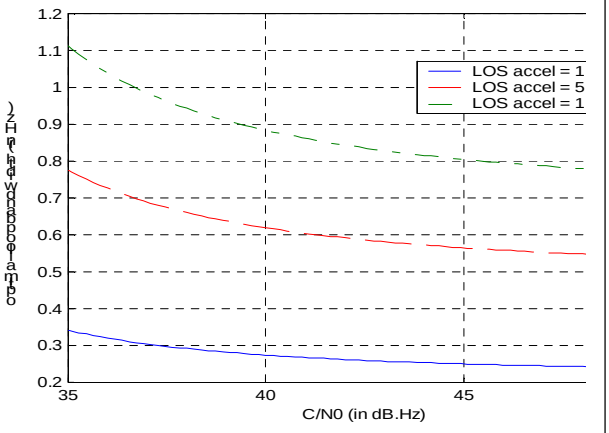

(b)

Figure II.1: Optimal loop bandwidth as a function of the LOS acceleration for several C/N_0 (a), and as a function of the C/N_0 for several LOS accelerations (b) for an unaided 2nd order early minus late DLL with a 20ms predetection

(68), the optimal setting is obtained if

$$|E_{\infty}(k)| + a.\sigma_b = L_{th} \quad (70)$$

This optimal condition can be written in function of the poles of the transfer function of the loop by inserting (65) and (66) in (70) as

$$\left|A_{IN}(k).G(p)\right| + a.\sqrt{\left\|E(z,p)\right\|_2^2}.\sigma_{eq} = L_{th} \quad (71)$$

Finally, the optimal multiple pole of the transfer function that minimizes the power of the thermal noise on the measurements is a solution of the equation

$$f(p) = 0 \quad (72)$$

with

$$f(p) = \left|A_{IN}(k).G(p)\right| + a.\sqrt{\left\|E(z,p)\right\|_2^2}.\sigma_{eq} - L_{th} \quad (73)$$

Moreover, as the ENB and the squared norm of $E(z)$ are conversely proportional with the pole (see figures I.7, I.8, I.11 and I.12), the solution that minimizes the ENB is the largest solution of (72) with the constraint that it stays in the stability range of the loop given in (27) for the PLL and in (54) for the DLL. When the loop is set with its optimal pole, the power of the random true error on the carrier phase or code delay measurements is minimized and

$$\sigma_{b_{OUT}}^2 = Bp.\left\|H(z,p_{opt})\right\|_2^2.\sigma_{eq}^2 = 2Bp.Bl_{p_{opt}}.\sigma_{eq}^2 \quad (74)$$

Optimal loop bandwidth has been plotted on figure II.1 as a function of the line of sight (LOS) acceleration and as a function of the C/N_0 ratio for the 2nd order DLL which is describe in the legend of the figure. It is necessary to estimate the two parameters σ_{eq}^2 and $A_{IN}(k)$ to build the function $f(p)$. These estimations can be obtained by observing the observable error signal $e(k)$. Its mean value divided by the SSEF at epoch k gives $A_{IN}(k)$ according to (66), and its variance divided by the squared norm of $E(z)$ gives σ_{eq}^2 according to (65). An easy and low cost method to estimate the mean value $\mu_e(k)$ and the variance $\sigma_e^2(k)$ of $e(k)$ at epoch k is to use two low-pass filters of order 1 defined by

$$\mu_e(k) = (1-b).e(k) + b.\mu_e(k-1) \quad (75)$$

and

$$\sigma_e^2(k) = (1-b).(e(k)-\mu_e(k))^2 + b.\sigma_e^2(k-1) \quad (76)$$

where b sets the time constant and the bandwidth of the low-pass filters. For information, the time of convergence (normalized by the sampling period) toward 95% of a constant input is

$$n_{95\%} = \frac{\ln(0.05)}{\ln(b)} \quad (77)$$

Then we can construct the function $f(p)$ and compute the optimal solution. To find the optimal zero of $f(p)$, we propose to use the iterative method of Newton-Raphson. An iteration is given by

$$p_{opt}(k+1) = p_{opt}(k) - \frac{f(p_{opt}(k))}{f'(p_{opt}(k))} \quad (78)$$

It is necessary to initialize the optimal pole value near to 1, which is the upper bound of the stability range of the loops, to find the largest stable solution. This method has good properties of convergence and is able to track the optimal solution even if the parameters of dynamic and noise are variable in time. As an illustration, results on figure II.1 have been computed by sweeping the LOS acceleration in (a) or the C/N0 in (b) over 100 iterations of (78). The function $f(p)$ and its derivative have been built at each iteration with the new parameters values, and then the new optimal solution has been updated with respect to (78). In the FAB loop, the optimal solution is updated at the rate of the loop, which corresponds to 50Hz in general. But if the parameters have slow variations, the update of the optimal solution can be done at a lower rate to decrease the calculation cost of the processor in the receiver. Note that the resulting transfer function of the FAB loop is variable with time because of the variability of its poles. E.I. JURY has shown in [4] that if the poles are not enough slowly variable, then the filter can produce important peak values in the time domain. In the FAB loop, these undesirable peaks could cause the error signal to be out of the lock range. For this reason, it is necessary to smooth the optimal pole of the FAB loop by a low-pass filter before updating the loop filter coefficients. In the case of quick rise of the dynamics, the time constant of the algorithm doesn't open the effective bandwidth of the loop as fast. As a consequence, a detection system has to

be inserted. We propose to watch the mean plus 3 sigma value of the error signal, which is the value of $f(p)$ minus L_{th} at the effective pole, and to suddenly open the loop bandwidth and re-initialize the algorithm if this value is greater than the upper bound of the lock range. In practical, the lower bound of the loop bandwidth is a function of the level of the phase noise of the NCOs. At low dynamics, the FAB algorithm provides low optimal loop bandwidth that could be under the lower bound if the NCOs are not good. In this case, the loop could not be set at its optimal values. As a conclusion, the different steps in one iteration of the FAB algorithm are: 1) To estimate the variance and the mean values of the observable error signal at the input of the loop filter as defined in (75) and (76); 2) To build the optimization function $f(p)$ defined in (73) with the appropriate expressions defined in section I; 3) To find its greater zero in the stability range with the Newton-Raphson method as defined in (78); 4) To smooth the optimal solution not to have undesirable peaks; 5) To update the loop filter coefficients with the appropriate expressions (as it was shown in section I) as a function of the optimal pole. Finally, the code delay or carrier phase measurement must be corrected by the estimation of the steady state error to cancel the bias due to dynamic.

III. RESULTS OF THE IMPLEMENTATION

A FAB loop has been implemented on a channel of the GEC-PLESSEY GPS-BUILDER. The GPS-BUILDER board is plugged on the PCI bus of a PC computer. The

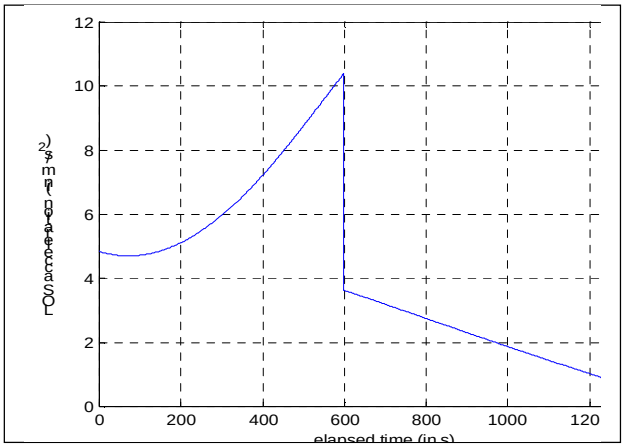

board performs the frequency down conversions of the received HF signal, the analog to digital conversion, and the mixing with a local in-phase and in-quadrature carrier and a local prompt and delayed code for 12 channels. The computer receives all these outputs integrated over 1ms, treats it and drives the NCOs and the local code generators. We have inserted our algorithm in the C code source of the software provided with the board. The signal has been simulated with the GLOBAL SIMULATION SYSTEMS 2760 GPS signal simulator. We have built an unaided second order FAB-DLL to support dynamics of order 2. The acceleration of the simulated vehicle has been set to 1g during 600s and to a small value from 600s till the end. The resultant LOS acceleration on the considered channel is plotted on figure III.1. The C/N_0 is over 45dB.Hz. The real-time FAB loop bandwidth is plotted on figure III.2. The initial loop bandwidth has been

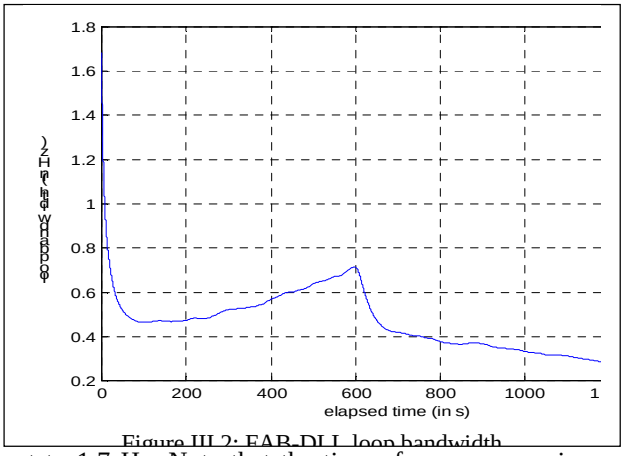

Figure III.2: FAB-DLL loop bandwidth

set to 1.7 Hz. Note that the time of convergence is over 60s due to the convergence of the estimators and to the smoothing of the optimal solution. After the convergence step, algorithm tracks the evolution of the acceleration and provides real-time optimal loop bandwidth.

IV. CONCLUSION

This paper has proposed a new systematic method to minimize the thermal noise error on code delay and carrier phase measurements using the FAB lock loops. Its robustness, which is due to a precise analytic study of the models of the loops, has been shown by a real initial implementation. As it depends on the variability of the signal parameters, various tests are actually performed to evaluate the efficiency of the algorithm on several realistic scenarios. Finally, the method is limited by the quality of the signals provided by the NCOs of the receiver, which fixes the lower bound of the loop bandwidth at low dynamics.

V. APPENDIX

A- Simplification of the linear model of an I&D-PLL

The inclusion of the I&D predetection filter model (figure

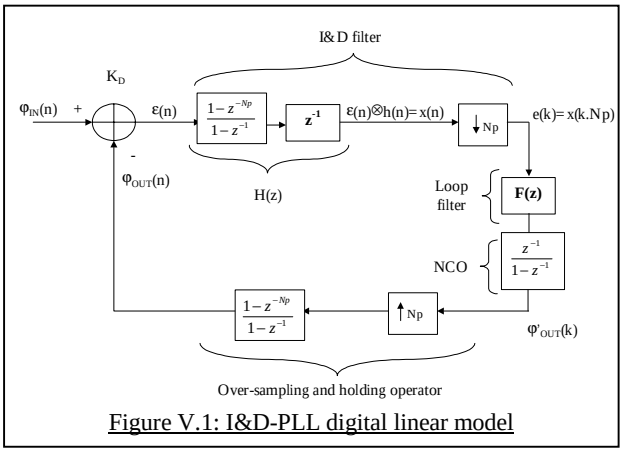

Figure V.1: I&D-PLL digital linear model

I.4) and of the holding operation model (figure I.5) in the generic loop model of figure I.3 provides the model shown on figure V.1. We will show that it is possible to simplify this multi-rate model. Let's write the error signal e(k) with respect to $\varphi_{IN}(n)$ and $\varphi_{OUT}(n)$:

$$e(k) = x(n)|_{n=k.Np} = \varepsilon(n) \otimes h(n)|_{n=k.Np} \quad (79)$$

$$\Leftrightarrow e(k) = K_D.[\ (\varphi_e(n) \otimes h(n))|_{n=k.Np} - (\varphi_s(n) \otimes h(n))|_{n=k.Np}\ ]$$

where K_D is the gain of the discriminator and

$$h(n) = TZ^{-1}\left[\frac{1-z^{-N}}{1-z^{-1}} \cdot z^{-1}\right] \quad (80)$$

According to (79), the digital linear model of the loop on figure V.1 is equivalent to the one that is showing on figure V.2. Finally, the branch between labels **A** and **B** in figure V.2 can be simplified as it is shown on figure V.3. We finally obtained the simplified digital linear model of the I&D-PLL (shown on figure I.6) by inserting the simplification of figure V.3 in figure V.2.

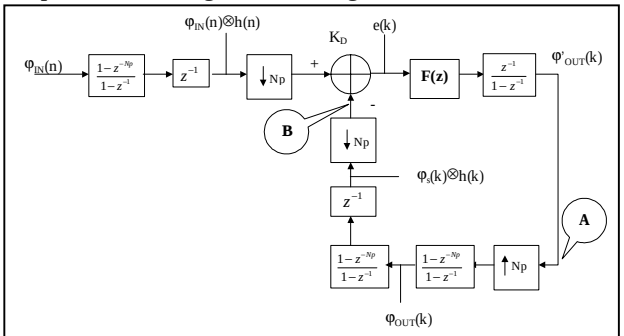

Figure V.2: First simplification of the I&D-PLL model

B- Calculation of the mean value over blocks of Np samples of the input phase

As an example, let's consider an input phase of order 2. So

$$\varphi_{IN}(t) = \sum_{m=0}^{2} \varphi_0^{(m)} . \frac{t^m}{m!} \quad (81)$$

The sampled version of (81) is

$$\varphi_{IN}(n) = \sum_{m=0}^{2} \varphi_0^{(m)} . \frac{n^m}{m!.{F_S}^m} \quad (82)$$

where F_S is the sampling frequency. Then, the mean value over the k^{th} block of *Np* samples of the input phase is

$$\langle \varphi_{IN}(n) \rangle_k = \sum_{m=0}^{2} \varphi_0^{(m)} . \frac{\langle n^m \rangle_k}{m!.{F_S}^m} \quad (83)$$

with

$$\langle n^m \rangle_k = \frac{1}{Np} \sum_{n=(k-1)Np}^{k.Np-1} n^m \quad (84)$$

The computation of (84) for the 3 terms of (83) results in

$$\begin{cases} \langle n^0 \rangle_k = 1; \langle n^1 \rangle_k = k.Np - \frac{1}{2}(Np+1) \\ \langle n^2 \rangle_k = k^2.Np^2 - k.Np(Np+1) + \frac{Np^2}{3} + \frac{Np}{2} + \frac{1}{6} \end{cases} \quad (85)$$

As the length of the accumulation window *Np* is the ratio between the sampling frequency F_S and the predection bandwidth B_p, insertion of equations of system (85) in (82) results in

$$\langle \varphi_{IN}(n) \rangle_k = \sum_{m=0}^{2} A_0^{(m)} . \frac{k^m}{m!} \quad (86)$$

where $A_0^{(m)}$ is defined as the equivalent initial value of the m^{th} derivative of the meaning input phase and

$$\begin{cases} A_0^{(0)} = \varphi_0^{(0)} - \frac{\varphi_0^{(1)}}{2B_p}\left(1 + \frac{1}{Np}\right) + \frac{\varphi_0^{(2)}}{2{B_p}^2}\left(\frac{1}{3} + \frac{1}{2Np} + \frac{1}{6Np^2}\right) \\ A_0^{(1)} = \frac{\varphi_0^{(1)}}{B_p} - \frac{\varphi_0^{(2)}}{2{B_p}^2}\left(1 + \frac{1}{Np}\right); \quad A_0^{(2)} = \frac{\varphi_0^{(2)}}{{B_p}^2} \end{cases}$$

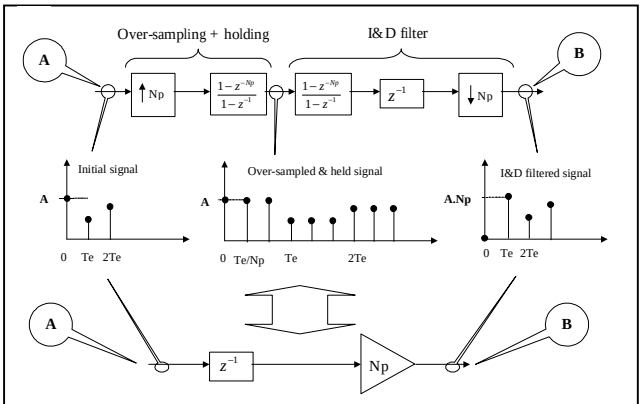

Figure V.3: Simplification of the feedback arm

If we consider that the rate *Np* between the sample frequency and the predetection bandwidth is larger than 1, then the system (87) can be approximated by

$$\begin{cases} A_0^{(0)} = \varphi_0^{(0)} - \frac{\varphi_0^{(1)}}{2B_p} + \frac{\varphi_0^{(2)}}{6{B_p}^2} \\ A_0^{(1)} = \frac{\varphi_0^{(1)}}{B_p} - \frac{\varphi_0^{(2)}}{2{B_p}^2}; A_0^{(2)} = \frac{\varphi_0^{(2)}}{{B_p}^2} \end{cases} \quad (88)$$

Finally, as the predetection bandwidth is greater than 1, we can approximate the equivalent initial value of the m^{th} derivative of the meaning input phase by

$$A_0^{(m)} \approx \frac{\varphi_0^{(m)}}{{B_p}^m} \quad (89)$$

REFERENCES

[1] E.D. KAPLAN - 'Understanding GPS, principles and applications' - Artech House - 1996

[2] W.C. LINDSEY, C.M. CHIE - 'A survey of digital phase-locked loops' - Proceeding of the IEEE, Vol. 69, No 4 - April 1981

[3] M.S. BRAASCH, A.J. VAN DIERENDONCK - 'GPS receiver architectures and measurements' - Proceedings of the IEEE, Vol. 87, No 1 - January 1999

[4] E.I. JURY - 'Theory and application of the *z* transform method' - Ed John Wiley & Sons, Inc. - 1964

ACKNOWLEDGMENTS

The authors wish to thank ASPI and CNES for supporting this research, and STNA for having provided technical assistance.